Dose–Effect Relationships of ^{166}Ho Radioembolization in Colorectal Cancer

Caren van Roekel*, Remco Bastiaannet*, Maarten L.J. Smits, Rutger C. Bruijnen, Arthur J.A.T. Braat, Hugo W.A.M. de Jong, Sjoerd G. Elias, and Marnix G.E.H. Lam

University Medical Center Utrecht, Utrecht University, Utrecht, The Netherlands

Radioembolization is a treatment option for colorectal cancer (CRC) patients with inoperable, chemorefractory hepatic metastases. Personalized treatment requires established dose thresholds. Hence, the aim of this study was to explore the relationship between dose and effect (i.e., response and toxicity) in CRC patients treated with ^{166}Ho radioembolization. **Methods:** CRC patients treated in the HEPAR II and SIM studies were analyzed. Absorbed doses were estimated using the activity distribution on posttreatment ^{166}Ho SPECT/CT. Metabolic response was assessed using the change in total-lesion glycolysis on ^{18}F-FDG PET/CT between baseline and 3-mo follow-up. Toxicity between treatment and 3 mo was evaluated according to the Common Terminology Criteria for Adverse Events (CTCAE), version 5, and its relationship with parenchyma-absorbed dose was assessed using linear models. The relationship between tumor-absorbed dose and patient- and tumor-level response was analyzed using linear mixed models. Using a threshold of 100% sensitivity for response, the threshold for a minimal mean tumor-absorbed dose was determined and its impact on survival was assessed. **Results:** Forty patients were included. The median parenchyma-absorbed dose was 37 Gy (range, 12–55 Gy). New CTCAE grade 3 or higher clinical and laboratory toxicity was present in 8 and 7 patients, respectively. For any clinical toxicity (highest grade per patient), the mean difference in parenchymal dose (Gy) per step increase in CTCAE grade category was 5.75 (95% CI, 1.18–10.32). On a patient level, metabolic response was as follows: complete response, $n = 1$; partial response, $n = 11$; stable disease, $n = 17$; and progressive disease, $n = 8$. The mean tumor-absorbed dose was 84% higher in patients with complete or partial response than in patients with progressive disease (95% CI, 20%–180%). Survival for patients with a mean tumor-absorbed dose of more than 90 Gy was significantly better than for patients with a mean tumor-absorbed dose of less than 90 Gy (hazard ratio, 0.16; 95% CI, 0.06–0.511). **Conclusion:** A significant dose–response relationship in CRC patients treated with ^{166}Ho radioembolization was established, and a positive association between toxicity and parenchymal dose was found. For future patients, it is advocated to use a ^{166}Ho scout dose to select patients and yo personalize the administered activity, targeting a mean tumor-absorbed dose of more than 90 Gy and a parenchymal dose of less than 55 Gy.

Key Words: radioembolization; holmium; dosimetry

J Nucl Med 2021; 62:272–279
DOI: 10.2967/jnumed.120.243832

Colorectal cancer (CRC) is one of the most common types of cancer worldwide (*1*). The liver is the first site of hematogenous spread, and 70%–80% of patients with hepatic metastases have disease that is deemed unresectable because of tumor size, location, multifocality, or inadequate hepatic reserve (*2*). Hence, in most patients, metastatic CRC cannot be cured. Palliative treatment generally consists of several lines of systemic chemotherapy. If the available chemotherapeutic options fail, treatment with radioembolization should be considered for patients with liver-only or liver-dominant disease (*3*).

During radioembolization, radioactive microspheres are delivered intraarterially to hepatic tumors. The rationale of this treatment is to administer a high local radiation dose to the tumors while relatively sparing the healthy liver parenchyma by using the predominant arterial blood flow to tumors. Currently, 3 types of microspheres are available: ^{90}Y resin microspheres (SIRspheres; Sirtex), ^{90}Y glass microspheres (TheraSphere; BTG/Boston Scientific), and ^{166}Ho microspheres (Quiremspheres; Quirem Medical).

One advantage of ^{166}Ho radioembolization is that treatment can be preceded by a scout dose of the same microspheres, using only limited activity (250 MBq). This ^{166}Ho scout dose has proven to be a more accurate predictor of the distribution of the treatment dose (*4*). Another advantage is that ^{166}Ho microspheres can be visualized by both MRI and SPECT/CT (*5*). The safety and efficacy of ^{166}Ho radioembolization were determined in the HEPAR and SIM studies (*6–9*). In these studies, activity calculation was based on a whole-liver absorbed dose of 60 Gy. To allow for personalized, or optimized, treatment, reference levels for efficacy and toxicity are needed (*10*). Hence, the aims of this study were to determine the relationship between dose and toxicity and between dose and metabolic response in CRC patients who are treated with ^{166}Ho radioembolization.

MATERIALS AND METHODS

Patients

This was a retrospective analysis of CRC patients who were treated with ^{166}Ho radioembolization in the HEPAR II study (NCT01612325 (*6*)) and the SIM study (NCT02208804 (*8*)). Before study inclusion, all patients provided written informed consent. The institution's Medical Ethics Committee approved both studies. The CRC patients of the

Received Feb. 21, 2020; revision accepted May 27, 2020.
For correspondence or reprints contact: Caren van Roekel, University Medical Center Utrecht, Heidelberglaan 100, 3584 CX Utrecht, The Netherlands.
E-mail: j.vanroekel@umcutrecht.nl
*Contributed equally to this work.
Published online Jun. 26, 2020.

HEPAR II study were already part of a preliminary mixed tumor-type cohort analysis and were also included in this CRC-only analysis (*11*).

Treatment Procedures

During work-up, laboratory and clinical examinations were performed and patients underwent multiphasic liver CT and ^{18}F-FDG PET/CT at a median of 16 d before treatment (range, 6–42 d). Pretreatment activity was calculated using a method similar to the MIRD method (*12*). The injected activity to reach an average absorbed dose of 60 Gy in the target volume was calculated as (*7*)...

$$\text{Injected activity (MBq)} = \text{target volume weight (kg)} \times 3,780 \left(\frac{\text{MBq}}{\text{kg}}\right).$$

The injected activity was not adjusted for lung shunt fraction, in line with the instructions for use for Quiremspheres. Since the abundance of γ-photons invokes detector dead-time, patients underwent quantitative ^{166}Ho SPECT/CT to assess the therapeutic dose distribution 3–5 d after treatment.

The threshold used for tumor delineation was defined per patient, based on twice the mean aortic blood-pool SUV corrected for lean body mass. Using this patient relative threshold and the volume restriction of 5 cm^3, tumors were automatically defined. In this way, only regions with metabolic activity significantly exceeding the background activity of the liver were defined. The threshold used to delineate tumors at follow-up was defined again on the 3-month ^{18}F-FDG PET/CT.

A rigid registration (using Elastix software (*13*)) of the CT scans from the PET and SPECT acquisitions was used to transfer the PET-based tumor and liver contours to the corresponding ^{166}Ho SPECT reconstructions. The previously manually contoured livers acted as a mask to focus registration on this region exclusively. All registration results were checked visually. Minor manual adjustments were allowed but were based only on CT and never on nuclear imaging. A 1-cm dilation of the tumor and liver contours was used, to account for breathing movement, errors in registration, and resolution differences. The counts in the dilated contours were used for activity calculation, but the volume of the nondilated volumes of interest was used for absorbed dose calculation. The quantitative Monte Carlo–based SPECT reconstruction used in this study yields voxels that contain absolute activity (in MBq). The absorbed dose (Gy) in each voxel was subsequently calculated using the local deposition model, which posits that at the resolution of SPECT, all dose is deposited within the voxel of origin. The average doses in parenchymal tissue and tumors was calculated using the transferred delineations, as described previously (Fig. 1) (*11*).

If there were fused lesions at follow-up, a volume-weighted average of the absorbed dose of the different components at baseline was calculated. Also, a weighted average, correcting for tumor volume, was calculated to obtain the mean tumor-absorbed dose per patient. The parenchyma-absorbed dose was determined using the activity in the entire (dilated) liver contour, with the activity in the dilated tumor regions subtracted.

Toxicity Evaluation

The emergence of clinical toxicity between treatment and 3 mo after treatment was recorded, with the exception of clinical adverse events during the first week after treatment, to allow for distinction between adverse events due to embolization and adverse events due to radiation. Laboratory toxicity between treatment and 3 mo after treatment was evaluated using the following parameters: albumin, alkaline phosphatase, alanine aminotransferase, aspartate aminotransferase, bilirubin, and γ-glutamyltransferase. Common Terminology Criteria for Adverse Events (CTCAE), version 5.0, were used for grading (*14*). Since version 5.0 allows for higher values of laboratory parameters when these were already abnormal at baseline, the relative change in laboratory values between baseline and the 3-mo follow-up was calculated as well. Furthermore, the presence of ascites and encephalopathy (as part of radioembolization-induced liver disease) was determined at the 3-mo follow-up.

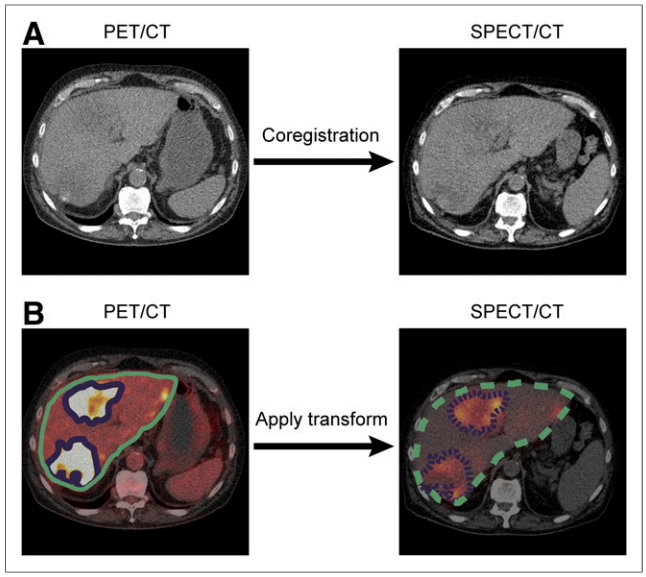

FIGURE 1. Example of tumor delineation and absorbed-dose estimation. (A) Using liver contour, low-dose CT of PET/CT was matched to low-dose CT of SPECT/CT. Tumors were automatically defined using threshold. (B) Liver and tumor contours were transferred from PET/CT to SPECT/CT, and absorbed doses were calculated.

Efficacy Evaluation

Metabolic response to treatment was evaluated on ^{18}F-FDG PET/CT at the 3-mo follow-up.

Tumors were automatically defined on the basis of SUV, and total-lesion glycolysis was determined. To avoid misidentification, baseline and follow-up images were evaluated in parallel. The metabolic response of hepatic lesions was defined on the basis of the change in total-lesion glycolysis between baseline and follow-up, according to PERCIST (*15*). Hepatic tumor response was also assessed according to RECIST, version 1.1 (*16*).

Statistical Analyses

Patient demographics and treatment characteristics were summarized using descriptive analyses. The strength of association between CTCAE toxicity grade and parenchyma-absorbed dose was assessed using linear regression models, with CTCAE grade in categories as the dependent continuous variable and parenchyma-absorbed dose as the independent continuous variable. For clinical significance, CTCAE grading of any clinical and laboratory toxicity was also dichotomized as grade 0/I/II or grade III/IV/V and analyzed using logistic regression with Firth correction for small-sample bias (*18*). The association between relative change in laboratory parameters and the dose to healthy liver tissue was analyzed using simple linear regression models, with percentage change as the dependent continuous variable and parenchyma-absorbed dose as the independent continuous variable, after log transformation of the dependent variable to fulfill model assumptions. All toxicity analyses were also adjusted for response to therapy (binary coded as response or nonresponse),

previous treatment (defined as number of prior systemic treatment lines, categoric variable), and tumor load (defined as percentage involvement of the liver by tumors, continuous variable) as possible confounders, which were identified by making directed acyclic graphs.

The relationship between tumor-absorbed dose and response was analyzed using a linear mixed-effects regression model, with tumor-absorbed dose as the dependent variable. This type of analysis was chosen to account for correlation of tumors within patients. To fulfill model assumptions, dose was log-transformed. Nested models were compared using the Akaike information criterion. The dose–effect relationship was best explained using a random intercept per patient without random slopes. A geometric mean of the tumor-absorbed dose per patient per response category was estimated because the anti-log of the arithmetic mean of log-transformed values is the geometric mean. A trend test was also done, with response as a continuous variable in the model, to test for the presence of an ordered relationship across response categories. Analyses were adjusted for the following possible confounders by including them as covariables: previous treatment (coded as factor with the following categories: previous treatment with anti–vascular endothelial growth factor [medication] [yes or no]) and tumor load (continuous). A receiver-operating-characteristic analysis, accounting for clustered data, was done to determine the discriminatory power of tumor dose in response estimation (*17*). The 95% confidence interval for the area under the curve shows the boundaries of the likely discriminative ability of tumor dose for response in this cohort. Using a threshold of 100% sensitivity for response (complete response [CR] or partial response [PR]), the threshold for a minimal mean tumor-absorbed dose was determined and used in the survival analyses. The same threshold of 100% sensitivity for response was used to determine the threshold for a minimal tumor-absorbed dose (lesion level).

The agreement between response according to PERCIST and according to RECIST was analyzed using the Cohen κ, with disagreements weighted according to their squared distance from perfect agreement.

Overall survival was defined as the interval between treatment and death from any cause. Cox regression models were made using Firth correction for small-sample bias (*18*). Analyses were adjusted for the following possible confounders: tumor load, parenchymal dose, and the presence of extrahepatic disease at baseline. Inspection of Schoenfeld residuals showed that the proportionality of the hazard assumption was not violated. Analyses were performed using R statistical software, version 3.6.2 for Microsoft Windows. The following R libraries were used: readxl, version 1.3.1; dplyr, version 0.8.3; data.table, version 1.12.8; lme4, version 1.1-21; nlme, version 3.1-143; ggplot2, version 3.2.1; gdata, version 2.18.0; gmodels, version 2.18.1; ggpubr, version 0.2.4; Hmisc, version 4.3-0; lmerTest, version 3.1.0; foreign, version 0.8-72; ggfortify, version 0.4.8; logistf, version 1.23; grid version, 3.6.2; car, version 3.0-5; pROC, version 1.15.3; ggeffects, version 0.14.0; splines, version 3.6.2; sjmisc, version 2.8.3; rel, version 1.4.1; and rcompanion, version 2.3.21. We report effect estimates with associated 95% CIs and corresponding 2-sided *P* values.

TABLE 1
Baseline Patient and Treatment Characteristics

Characteristic	Data
Sex	
Male	25 (62.5)
Female	15 (37.5)
Age (y)	64 (37–84)
World Health Organization performance score	
0	28 (70)
1	11 (27.5)
2	1 (2.5)
Previous locoregional (liver) therapy*	
External-beam radiation therapy	2 (5)
Metastasectomy	5 (12.5)
Radiofrequency ablation	3 (7.5)
Lines of prior systemic treatment	
1	8 (20)
2	20 (50)
3	7 (17.5)
4	5 (12.5)
Extrahepatic disease before treatment	
Lymph node	10 (25)
Lung	10 (25)
No	23 (57.5)
Liver volume (cm^3)	1,987 (1,272–3,167)
Metabolic tumor volume (cm^3)	320 (26–1,446)
Fractional tumor load	0.15 (0.01–0.49)
Radioembolization treatment	
Whole-liver	39 (97.5)
Lobar (right lobe only)	1 (2.5)
Administered activity (MBq)	6,387 (3,822–12,386)

*No patient received synchronous systemic treatment.
Qualitative data are numbers and percentages; continuous data are median and range.

RESULTS

Forty patients were included, with a total of 133 hepatic lesions. Three patients did not have follow-up imaging for tumor response assessment and were included in only the survival and toxicity analyses. Patient and treatment characteristics are summarized in Table 1.

Toxicity

The median parenchyma-absorbed dose was 37 Gy (range, 12–55 Gy). Toxicity during the 3 mo after treatment and CTCAE grades are summarized in Table 2. New clinical toxicity of at least grade 3 was present in 8 patients (20%), and new laboratory toxicity of at least grade 3 was present in 7 patients (17.5%). There was 1 patient (2.5%) who developed radioembolization-induced liver disease, evidenced by hyperbilirubinemia, hypoalbuminemia, and ascites, without evidence of progression or biliary obstruction. The mean parenchyma-absorbed dose of this patient was 34 Gy.

The results of the linear clinical toxicity regression analyses suggested a positive association between higher parenchymal dose and increase in the CTCAE grade for clinical toxicity (Supplemental Table 1; supplemental materials are available at http://jnm.snmjournals.org). The mean difference in parenchymal dose for patients with any clinical toxicity of CTCAE grade 0, 1, or 2 versus 3, 4, or 5 was 11.6 Gy (95% CI, 3.4–19.7; $P = 0.0070$). The odds ratio for any clinical toxicity of CTCAE grade 3, 4, or 5 versus 0, 1, or 2 per 10-Gy increase in parenchymal

TABLE 2
CTCAE Grading of New Clinical Toxicity per Patient During the 3 Months After Treatment

Toxicity	CTCAE grade I	CTCAE grade II	CTCAE grade III	CTCAE grade IV	CTCAE grade V
Abdominal pain	16	10	4		
Nausea	15	9	2		
Fatigue	21	10	2		
Anorexia	10	5			
Dyspnea	4	1			
Fever	7	1	1		
Ascites	1		2		
Flulike symptoms	2	1			
Malaise	4	1			
Hepatic failure			1		1*
Weight loss	2				
Chest pain	1	2			
Vomiting	9	5			
Dyspepsia	1	1			
Metal taste	3				
Contrast allergy	1	2			
Hematoma	1				
Diarrhea	1				
Constipation	4				
Upper gastrointestinal tract bleeding			1		
Limb edema	2				
Dizziness	1				
Chills	2				
Any clinical toxicity	13	19	7		1
Lowered albumin	9	4			
Elevated alanine aminotransferase	24	1	1		
Elevated alkaline phosphatase	4	14	2		
Elevated aspartate aminotransferase	28	2			
Elevated bilirubin	2	1		2	
Elevated γ-glutamyltransferase	5	15	5		
Any laboratory toxicity	7	23	5	2	

*Radioembolization-induced liver disease.
Highest CTCAE grades per clinical symptom or laboratory value are represented.

dose was 7.62 (95% CI, 1.95–249.03; $P = 0.0063$) (Supplemental Table 2).

For laboratory toxicity, the results of the linear regression analyses for both the CTCAE grades and the relative change in laboratory parameters showed that a higher parenchyma-absorbed dose relates to an increase in laboratory toxicity (Supplemental Table 3; Fig. 2).

Efficacy

Solely based on the metabolic response of measurable hepatic metastases at baseline, there was 1 patient with CR, 11 with PR, 17 with stable disease, and 8 with progressive disease (PD) at the 3-mo follow-up. On a lesion level, CR occurred in 23 lesions, PR in 20 lesions, stable disease in 49 lesions, and PD in 23 lesions. A significant dose–response relationship was found on a patient and tumor level. The mean tumor-absorbed dose was 77% higher in patients with CR or PR than in patients with PD (95% CI, 18%–164%; $P = 0.011$), and the mean absorbed dose was 95% higher in patients with CR than in patients with PD (34%–188%, $P = 0.00065$) (Table 3). Mean absorbed doses per response category are shown in Figure 3. On the basis of the receiver-operating-characteristic analysis, the ability of tumor-absorbed dose to discriminate between patients with and without metabolic response was 0.671 (95% CI, 0.54–0.80) and the ability of mean tumor-absorbed dose per patient to differentiate between responders and nonresponders was 0.698 (95% CI, 0.45–0.95) (Fig. 4). At a mean tumor-absorbed dose threshold with 100% sensitivity (95% CI, 48%–100%) for CR or PR at a patient level (90 Gy), specificity was 38% (95% CI, 21%–56%). At a tumor level,

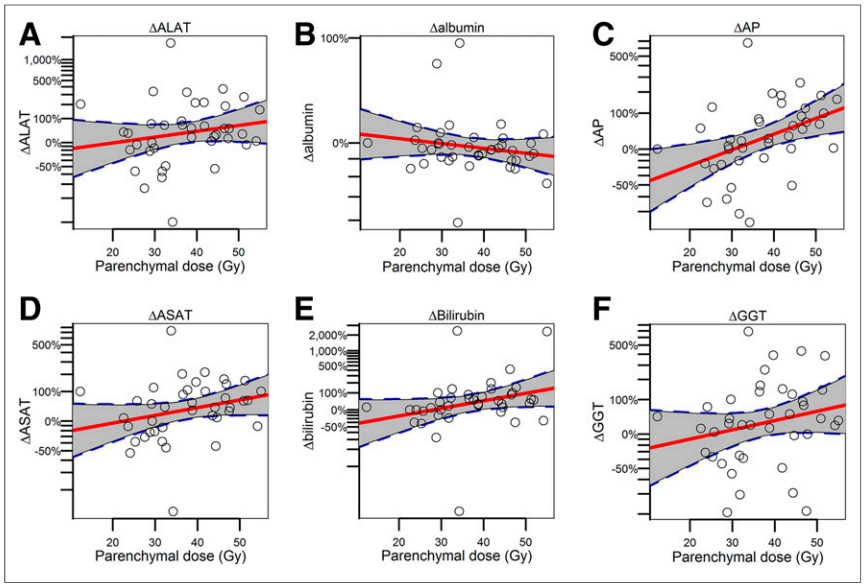

FIGURE 2. Association between change in laboratory parameters and parenchyma-absorbed dose. Red lines are regression lines, with 95% CIs indicated as surrounding gray areas. ALAT = alanine aminotransferase; AP = alkaline phosphatase; ASAT = aspartate aminotransferase; GGT = γ-glutamyltransferase.

without accounting for clustered data, sensitivity was 100% using a tumor-absorbed dose threshold of 80 Gy (95% CI, 74%–100%) and specificity was 41% (95% CI, 31%–51%). Agreement between PERCIST and RECIST was minimal, with a κ value of 0.345 (95% CI, 0.14–0.55). Anatomic response was lower than metabolic response in 15 cases (40.5%) and higher in 7 cases (18.9%).

Survival

Median overall survival was 10.7 mo (95% CI, 7.2–13.4). Survival differed significantly between patients without a metabolic response (including the development of new intra- or extrahepatic lesions) and patients with a metabolic response (hazard ratio, 2.34; 95% CI, 1.09–5.69; $P = 0.029$). After adjusting for tumor load, extrahepatic disease at baseline, and parenchymal dose, the hazard ratio for nonresponders was 2.54 (95% CI, 1.13–6.52; $P = 0.023$). Median overall survival in responders was 14.8 mo (95% CI, 14.2 mo–∞; $n = 8$) versus 8.6 mo (95% CI, 6.4–13.4 mo; $n = 29$) in nonresponders (Fig. 5). Furthermore, there was a significant difference in overall survival between patients with a mean tumor-absorbed dose of more than 90 Gy and patients with a mean tumor-absorbed dose of less than 90 Gy (hazard ratio, 0.16; 95% CI, 0.06–0.511; $P = 0.0031$; Fig. 6).

DISCUSSION

Building on the establishment—by Bastiaannet et al. (*11*)—of a dose–response relationship in patients treated with ^{166}Ho radioembolization, this study explored the dose–response relationship in a homogeneous population of patients with CRC only. Furthermore, dose–toxicity relationships were studied. Our results suggest a positive association between a higher parenchyma-absorbed dose and an increase in CTCAE grade, both for clinical and for laboratory toxicity. Furthermore, our data unveil, both at a lesion level and at a patient level, a significant dose–response relationship. Also, a mean tumor-absorbed dose of more than 90 Gy—the minimal mean tumor-absorbed dose in the group of patients with CR or PR—was associated with a significantly longer survival.

In this study, treatment with radioembolization was well tolerated. The most frequent clinical adverse events were abdominal pain, nausea, and fatigue of CTCAE grade 1 or 2. These

TABLE 3
Percentage Change in Mean Absorbed Dose per Response Category

Level	PR	Stable disease	PR	CR*	*P* (trend)
Patient level without new lesions	$n = 8$	$n = 17$	$n = 11$	$n = 1$	
Unadjusted	Reference	53.8 (5.6–24.2)	74.6 (18.6–57.6)	—	0.012
Adjusted†	Reference	62.0 (10.4–136.0)	77.3 (18.3–163.6)	—	0.019
Patient level with new lesions‡	$n = 23$	$n = 6$	$n = 7$	$n = 1$	
Unadjusted	Reference	29.8 (−15.1–98.6)	44.4 (1.4–106.0)	—	0.041
Adjusted†	Reference	18.7 (−24.3–85.4)	38.1 (−5.8–101.9)	—	0.12
Tumor level	$n = 23$	$n = 49$	$n = 20$	$n = 23$	
Unadjusted	Reference	31.1 (−3.2–78.8)	71.5 (17.1–150.4)	95.2 (34.7–183.6)	0.00030
Adjusted	Reference	35.2 (0.2–87.5)	72.2 (16.6–151.3)	94.8 (33.9–188.4)	0.00068

*As there was only 1 patient with complete metabolic response, categories CR and PR were taken together at patient level.
†Analyses were adjusted for previous treatment and tumor load or tumor volume (tumor-level analyses).
‡In which case patients were categorized as having PR.
Data are in grays, with 95% CIs in parentheses. For interpretation at tumor level, average dose is 95.23% higher in CR than PD (95% CI, 4.69%–183.62%).

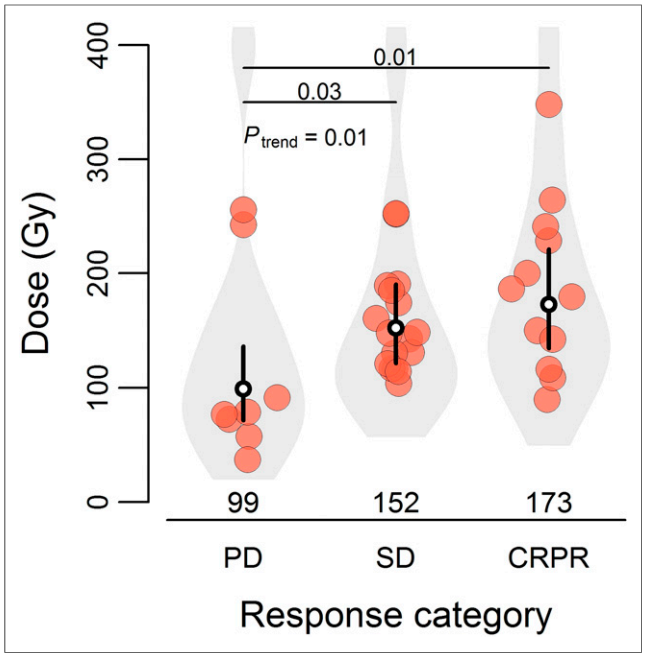

FIGURE 3. Relationship between mean tumor-absorbed dose per patient and metabolic response to treatment at 3-mo follow-up. Bullets show mean tumor-absorbed dose per patient. Black vertical lines are 95% CIs of mean doses per response category, with white dot in middle indicating mean tumor-absorbed dose per response category. This figure is based on unadjusted linear mixed-effects regression model as described in Table 3. CRPR = complete or partial response.

adverse events are well-known side effects of treatment with radioembolization (*19*). One patient of our study died of hepatic failure. This safety profile is compliant with the results of the MORE study, which showed that treatment with ^{90}Y resin radioembolization is safe in a patient population highly comparable to ours, namely CRC patients who received several lines of prior chemotherapy (*20*). A study on the safety of ^{90}Y glass radioembolization in CRC patients showed similar results, with the most frequent side effects being fatigue, abdominal pain, and nausea (*21*). The incidence of grade 3 or higher laboratory toxicity is also comparable among the 3 types of microspheres (*20,21*).

Regarding efficacy, the metabolic response rate (CR or PR) at the tumor level was 36%, comparable to previous dose–response data on resin microspheres in a similar patient cohort treated in the same hospital (*22*). In other studies, higher tumor response rates of up to 75% were found, with dose thresholds of 46 and 60 Gy (*23,24*). However, it is difficult to compare these studies with our study, as those patients were less heavily pretreated or received concomitant systemic therapy (*23,24*). Also, their thresholds cannot be compared with our data, as there are major differences in specific activity, size, number of particles, and half-life between microsphere types. There was only minimal agreement in response between the PERCIST and the RECIST assessments. In 15 patients of our study, RECIST underestimated response according to PERCIST. This finding is in accordance with other studies comparing these response assessments after radioembolization (*25,26*). Metabolic response assessment is not hampered by the presence of necrosis, cystic changes, and hemorrhage, as can be the case with size evaluation on transaxial images (*27*). Moreover, several studies found that changes in functional metrics, such as total-lesion glycolysis, were related to overall survival and were more accurate predictors than anatomic changes (*22,27,28*).

Although most of our patients underwent at least 2 prior lines of systemic treatment, the response rate seems suboptimal. Before treatment, patients with CRC are currently selected on the basis of clinical criteria, such as World Health Organization performance status and PR after several lines of chemotherapy (*29*). If patients are deemed eligible for treatment with radioembolization, a second selection criterion should be the activity distribution based on either ^{99m}Tc-macroaggregated albumin imaging or a ^{166}Ho scout dose. In view of the results of this study, we would argue that patients should be selected for treatment only if there is a favorable activity distribution with a sufficient mean tumor-absorbed dose of more than 90 Gy and a parenchyma-absorbed dose of less than 55 Gy. Although a causal relationship cannot be claimed solely on the basis of these observational data, the findings of this study suggest that below a mean tumor-absorbed dose of 90 Gy, metabolic response seems unlikely. However, since the discriminatory power of absorbed dose for response is limited, this number should be used with caution.

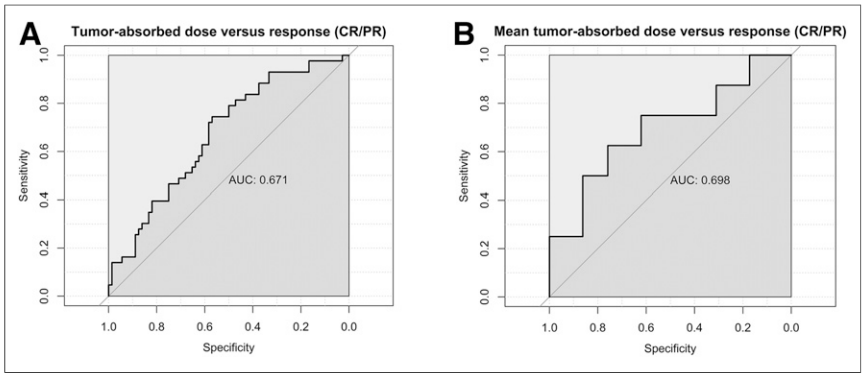

FIGURE 4. Receiver-operating-characteristic curve showing discriminative value of tumor-absorbed dose for response (A) and ability of mean tumor-absorbed dose per patient to discriminate between patients with CR or PR vs. stable disease or PD (B). AUCs are based on clustered data analysis; however, receiver-operating-characteristic curves are not.

The need for personalized dosimetry is widely accepted, with several studies showing a dose–response relationship in CRC patients treated with ^{90}Y resin radioembolization (*22–24,28*). There also is growing evidence for the possibility of improving treatment outcomes using personalized treatment planning in radioembolization (*10,11*). However, thus far, the DOSISPHERE study was the only study implementing personalized radioembolization planning in a prospective clinical study, investigating the tumor-absorbed dose and response rate in hepatocellular carcinoma patients using a standard versus a personalized dosimetric approach with ^{90}Y glass microspheres. Preliminary

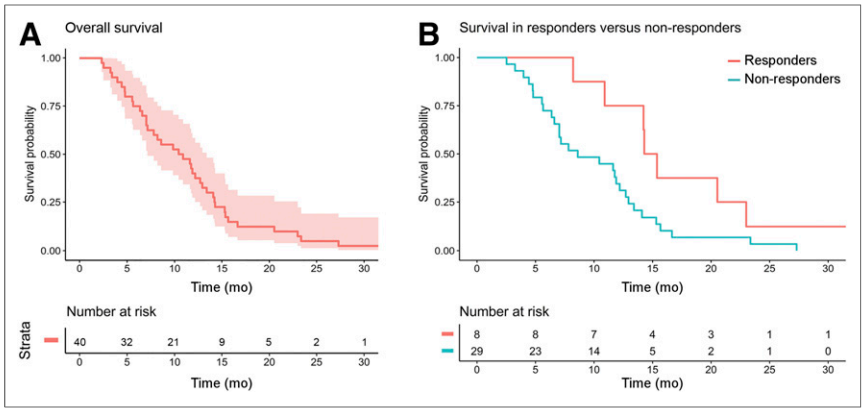

FIGURES 5. (A) Overall survival curve. (B) Survival curves for patients with and without metabolic response (including development of new lesions) at 3 mo.

results showed that both the response rates and the tumor-absorbed doses were significantly higher in the personalized dosimetry arm (*30*).

Strengths of this study were the homogeneous patient population, the standardized methods for tumor delineation, the use of a mixed-effects regression model accounting for clustered data, and the analyses of both safety and efficacy. This study also had several limitations. First, it was a single-center retrospective evaluation and there was a level of subjectivity in identifying the response of existing lesions, possibly leading to interoperator variations in estimated doses. Second, the sample size was limited and, because of the low incidence of toxicity, there were not enough data to allow us to draw a strong conclusion on the maximum tolerable parenchymal dose. Furthermore, the discriminatory value of absorbed dose for response estimation is limited, and a causal dose–response relationship cannot be claimed on the basis of these observational data. Hence, the reference values obtained should be interpreted with the uttermost caution and be used only as a direction. The rigid coregistrations applied in this study were likely affected by differences in patient positioning, differences in breath-hold policy, and the relatively low resolution of the low-dose CT component of the SPECT/CT. The resulting local errors are likely to propagate as underestimated tumor doses and as slightly overestimated parenchymal doses, thus contributing to the error in each response category and decreasing the statistical power.

In future studies on radioembolization in CRC patients, personalized dosimetry should be used. By using dosimetry-based optimized treatment planning, treatment doses can be tailored to the individual patient to acquire a maximum response while minimizing the chance of toxicity. As the incidence of toxicity was low, it is difficult to establish an absolute threshold for a maximum parenchymal dose. At the same time, it is likely that the parenchyma-absorbed dose threshold is different for each patient, dependent on many clinical characteristics. We therefore advise a pragmatic and clinically feasible approach, with activity calculation in order to obtain a sufficient tumor-absorbed dose and a parenchyma-absorbed dose of up to 55 Gy, dependent on individual patient characteristics. With a median parenchyma-absorbed dose of 37 Gy and a maximum of 55 Gy, this approach was proven to be safe, with only 1 case of radioembolization-induced liver disease. Furthermore, those patients for whom no meaningful mean tumor-absorbed dose (>90 Gy) can be reached at an acceptable parenchyma-absorbed dose threshold should be excluded from radioembolization treatment. On a tumor level, based on our results, treatment strategy should be adjusted to guarantee a tumor-absorbed dose of at least 80 Gy for every tumor. Partition modeling and multiple injection positions can be used to reach that objective. In other words, planning should be based primarily on applying a safe parenchyma-absorbed dose threshold, and patient selection should be based primarily on a sufficient tumor-absorbed dose.

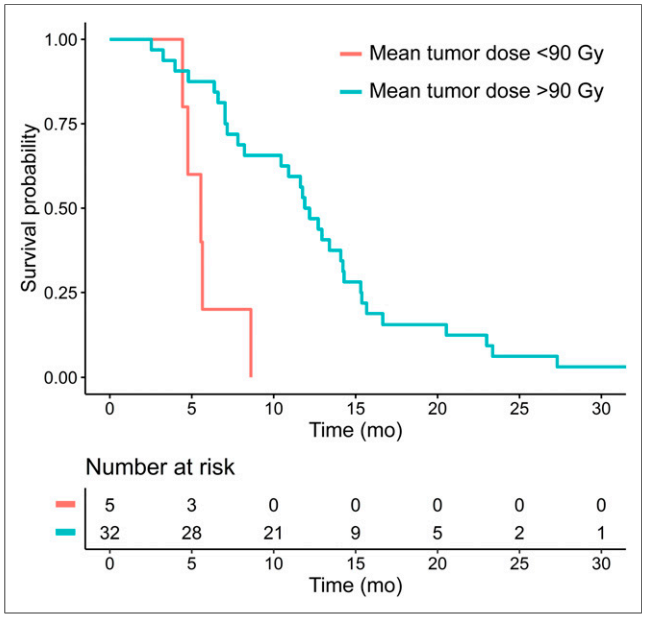

FIGURE 6. Survival curves for patients with higher (>90 Gy) or lower (<90 Gy) mean tumor-absorbed dose.

CONCLUSION

In CRC patients treated with ^{166}Ho radioembolization, a positive association between tumor-absorbed dose and metabolic response was established. Survival for patients with a mean tumor-absorbed dose of more than 90 Gy was significantly better than for patients with a mean tumor-absorbed dose of less than 90 Gy. There also was a positive association between parenchyma-absorbed dose and both laboratory and clinical toxicity. A treatment approach with selection of patients based on the activity distribution of the ^{166}Ho scout dose and personalized treatment activity calculation is advocated.

DISCLOSURE

Marnix Lam is a consultant for Boston Scientific and Terumo. Maarten Smits and Arthur Braat have served as speakers for BTG and Terumo. The Department of Radiology and Nuclear Medicine of the UMC Utrecht receives royalties from Quirem Medical and research support from Terumo and Quirem Medical.

No other potential conflict of interest relevant to this article was reported.

KEY POINTS

QUESTION: What is the relationship between dose and effect (i.e., response and toxicity) in CRC patients treated with ^{166}Ho radioembolization?

PERTINENT FINDINGS: A significant dose–response relationship was established. A positive relationship was found between parenchyma-absorbed dose and toxicity. A mean tumor-absorbed dose of more than 90 Gy was associated with improved overall survival.

IMPLICATIONS FOR PATIENT CARE: For future patients, it is advocated to use a ^{166}Ho scout dose to select patients and to personalize the administered activity, targeting a mean tumor-absorbed dose of more than 90 Gy.

REFERENCES

1. Bray F, Ferlay J, Soerjomataram I, Siegel RL, Torre LA, Jemal A. Global cancer statistics 2018: GLOBOCAN estimates of incidence and mortality worldwide for 36 cancers in 185 countries. *CA Cancer J Clin.* 2018;68:394–424.
2. Donadon M, Ribero D, Morris-Stiff G, Abdalla EK, Vauthey JN. New paradigm in the management of liver-only metastases from colorectal cancer. *Gastrointest Cancer Res.* 2007;1:20–27.
3. Colon cancer: version 1.2018. National Comprehensive Cancer Network website. https://oncolife.com.ua/doc/nccn/Colon_Cancer.pdf. Published January 18, 2019. Accessed September 16, 2019.
4. Smits MLJ, Dassen MG, Prince JF, et al. The superior predictive value of ^{166}Ho-scout compared with ^{99m}Tc-macroaggregated albumin prior to ^{166}Ho-microspheres radioembolization in patients with liver metastases. *Eur J Nucl Med Mol Imaging.* 2020;47:798–806.
5. Reinders MTM, Smits MLJ, van Roekel C, Braat A. Holmium-166 microsphere radioembolization of hepatic malignancies. *Semin Nucl Med.* 2019;49:237–243.
6. Prince JF, van den Bosch M, Nijsen JFW, et al. Efficacy of radioembolization with ^{166}Ho-microspheres in salvage patients with liver metastases: a phase 2 study. *J Nucl Med.* 2018;59:582–588.
7. Smits MLJ, Nijsen JFW, van den Bosch MAAJ, et al. Holmium-166 radioembolisation in patients with unresectable, chemorefractory liver metastases (HEPAR trial): a phase 1, dose-escalation study. *Lancet Oncol.* 2012;13:1025–1034.
8. van den Hoven AF, Prince JF, Bruijnen RC, et al. Surefire infusion system versus standard microcatheter use during holmium-166 radioembolization: study protocol for a randomized controlled trial. *Trials.* 2016;17:520.
9. Braat AJAT, Bruijnen RCG, van Rooij R, et al. Additional holmium-166 radioembolisation after lutetium-177-dotatate in patients with neuroendocrine tumour liver metastases (HEPAR PLuS): a single-centre, single-arm, open-label, phase 2 study. *Lancet Oncol.* 2020;21:561–570.
10. Kafrouni M, Allimant C, Fourcade M, et al. Retrospective voxel-based dosimetry for assessing the ability of the body-surface-area model to predict delivered dose and radioembolization outcome. *J Nucl Med.* 2018;59:1289–1295.
11. Bastiaannet R, van Roekel C, Smits MLJ, et al. First evidence for a dose-response relationship in patients treated with ^{166}Ho-radioembolization: a prospective study. *J Nucl Med.* 2020;61:608–612.
12. Salem R, Thurston KG. Radioembolization with ^{90}yttrium microspheres: a state-of-the-art brachytherapy treatment for primary and secondary liver malignancies. Part 1: technical and methodologic considerations. *J Vasc Interv Radiol.* 2006; 17:1251–1278.
13. Klein S, Staring M, Murphy K, Viergever MA. Elastix: a toolbox for intensity-based medical image registration. *IEEE Trans Med Imaging.* 2010;29:196–205.
14. *Common Terminology Criteria for Adverse Events (CTCAE): Version 5.0.* National Cancer Institute; 2018.
15. O JH, Lodge MA, Wahl RL. Practical PERCIST: a simplified guide to PET response criteria in solid tumors 1.0. *Radiology.* 2016;280:576–584.
16. Eisenhauer EA, Therasse P, Bogaerts J, et al. New response evaluation criteria in solid tumours: revised RECIST guideline (version 1.1). *Eur J Cancer.* 2009;45: 228–247.
17. Obuchowski NA. Nonparametric analysis of clustered ROC curve data. *Biometrics.* 1997;53:567–578.
18. Heinze G, Dunkler D. Avoiding infinite estimates of time-dependent effects in small-sample survival studies. *Stat Med.* 2008;27:6455–6469.
19. Riaz A, Awais R, Salem R. Side effects of yttrium-90 radioembolization. *Front Oncol.* 2014;4:198.
20. Kennedy AS, Ball D, Cohen SJ, et al. Multicenter evaluation of the safety and efficacy of radioembolization in patients with unresectable colorectal liver metastases selected as candidates for ^{90}Y resin microspheres. *J Gastrointest Oncol.* 2015;6:134–142.
21. Hickey R, Lewandowski RJ, Prudhomme T, et al. ^{90}Y radioembolization of colorectal hepatic metastases using glass microspheres: safety and survival outcomes from a 531-patient multicenter study. *J Nucl Med.* 2016;57:665–671.
22. van den Hoven AF, Rosenbaum CE, Elias SG, et al. Insights into the dose-response relationship of radioembolization with resin ^{90}Y-microspheres: a prospective cohort study in patients with colorectal cancer liver metastases. *J Nucl Med.* 2016;57:1014–1019.
23. Flamen P, Vanderlinden B, Delatte P, et al. Multimodality imaging can predict the metabolic response of unresectable colorectal liver metastases to radioembolization therapy with yttrium-90 labeled resin microspheres. *Phys Med Biol.* 2008;53:6591–6603.
24. Levillain H, Duran Derijckere I, Marin G, et al. ^{90}Y-PET/CT-based dosimetry after selective internal radiation therapy predicts outcome in patients with liver metastases from colorectal cancer. *EJNMMI Res.* 2018;8:60.
25. Jongen JMJ, Rosenbaum C, Braat M, et al. Anatomic versus metabolic tumor response assessment after radioembolization treatment. *J Vasc Interv Radiol.* 2018;29:244–253.e2.
26. Sager S, Akgun E, Uslu-Besli L, et al. Comparison of PERCIST and RECIST criteria for evaluation of therapy response after yttrium-90 microsphere therapy in patients with hepatocellular carcinoma and those with metastatic colorectal carcinoma. *Nucl Med Commun.* 2019;40:461–468.
27. Bastiaannet R, Lodge MA, de Jong H, Lam M. The unique role of fluorodeoxyglucose-PET in radioembolization. *PET Clin.* 2019;14:447–457.
28. Willowson KP, Hayes AR, Chan DLH, et al. Clinical and imaging-based prognostic factors in radioembolisation of liver metastases from colorectal cancer: a retrospective exploratory analysis. *EJNMMI Res.* 2017;7:46.
29. Dendy MS, Ludwig JM, Kim HS. Predictors and prognosticators for survival with yttrium-90 radioembolization therapy for unresectable colorectal cancer liver metastasis. *Oncotarget.* 2017;8:37912–37922.
30. Garin E. A multicentric and randomized study demonstrating the impact of MAA based dosimetry on tumor response in SIRT for HCC. GEST 2019 website. https://www.eventscribe.com/2019/GEST/fsPopup.asp?Mode=presInfo&PresentationID=521844. Presented May 10, 2019. Accessed September 16, 2020.